# Constitutively Active Arabidopsis MAP Kinase 3 Triggers Defense Responses Involving Salicylic Acid and SUMM2 Resistance Protein[1]

**Baptiste Genot, Julien Lang, Souha Berriri, Marie Garmier, Françoise Gilard, Stéphanie Pateyron, Katrien Haustraete, Dominique Van Der Straeten, Heribert Hirt, and Jean Colcombet***

Institute of Plant Sciences Paris Saclay, Centre National de la Recherche Scientifique, Institut National de Recherche Agronomique, Université Paris-Sud, Université Evry, Université Paris-Saclay, Paris Diderot, Sorbonne Paris-Cité, 91405 Orsay, France (B.G., J.L., S.B., M.G., F.G., S.P., H.H., J.C.); Laboratory of Functional Plant Biology, Ghent University, B-9000 Ghent, Belgium (K.H., D.V.D.S.); and Center for Desert Agriculture, King Abdullah University of Sciences and Technology, Thuwal 23955-6900, Saudi Arabia (H.H.)

**ORCID IDs: 0000-0001-9070-1772 (B.G.); 0000-0001-6043-4730 (S.B.); 0000-0002-6035-9993 (M.G.); 0000-0002-7755-1420 (D.V.D.S.); 0000-0003-3119-9633 (H.H.); 0000-0002-0176-3857 (J.C.).**

Mitogen-activated protein kinases (MAPKs) are important regulators of plant immunity. Most of the knowledge about the function of these pathways is derived from loss-of-function approaches. Using a gain-of-function approach, we investigated the responses controlled by a constitutively active (CA) MPK3 in *Arabidopsis thaliana*. *CA-MPK3* plants are dwarfed and display a massive derepression of defense genes associated with spontaneous cell death as well as the accumulation of reactive oxygen species, phytoalexins, and the stress-related hormones ethylene and salicylic acid (SA). Remarkably *CA-MPK3*/*sid2* and *CA-MPK3*/*ein2-50* lines, which are impaired in SA synthesis and ethylene signaling, respectively, retain most of the *CA-MPK3*-associated phenotypes, indicating that the constitutive activity of MPK3 can bypass SA and ethylene signaling to activate defense responses. A comparative analysis of the molecular phenotypes of *CA-MPK3* and *mpk4* autoimmunity suggested convergence between the MPK3- and MPK4-guarding modules. In support of this model, *CA-MPK3* crosses with *summ1* and *summ2*, two known suppressors of *mpk4*, resulted in a partial reversion of the *CA-MPK3* phenotypes. Overall, our data unravel a novel mechanism by which the MAPK signaling network contributes to a robust defense-response system.

To survive under different stresses during their life cycle, plants have developed various strategies. Their ability to adapt to changing environments largely relies on sensing and signaling processes that are based on manifold receptors and complex signaling networks. Mitogen-activated protein kinase (MAPK) cascades were shown to be key actors in plant signal transduction in response to various biotic and abiotic stresses (Colcombet and Hirt, 2008). The core of the MAPK pathways is formed by three types of kinases: MAPKK kinases (MAP3Ks), MAPK kinases (MAP2Ks), and MAP kinases (MAPKs), which phosphorylate and activate each other in a linear pathway. MAPKs, which are Ser/Thr kinases, are known to phosphorylate a wide range of substrates, including other kinases and transcription factors, leading to major stress-related cellular modifications. These three sets of protein kinases in MAPK pathways are encoded by multigene families (Ichimura et al., 2002). There are more than 60 MAP3Ks, 10 MAP2Ks, and 20 MAPKs in *Arabidopsis thaliana*, which define functional modules for multiple processes, including development and stress responses.

Interestingly, a given stress does not activate a single MAPK module. For example, the microbe-associated molecular pattern (MAMP) flg22, a derived peptide from *Pseudomonas aeruginosa* flagellin that reveals the presence of the pathogen to the plant, triggers the activation of several MAPKs: MPK3, MPK4, MPK6, MPK11, MPK1, and MPK13 (Meng and Zhang, 2013; Nitta et al., 2014). This activation occurs within minutes after flg22 perception by its cognate receptor complex FLS2-BAK1, peaking around 15 min and getting back to its basal level after 1 h (Nuhse et al., 2000; Asai et al., 2002). Upstream activators of the MAPKs also have been identified

[1] This work was supported by the Institut National de Recherche Agronomique, the Agence Nationale de la Recherche, and LabEx Saclay Plant Sciences (grant no. ANR-10-LABX-0040-SPS), managed by the French National Research Agency under the Investments for the Future program (grant no. ANR-11-IDEX-0003-02), by the French Ministry of Research (Ph.D. fellowship to B.G.), and by the Research Foundation Flanders (grant no. FWO G.0656.13N to D.V.D.S.) and Ghent University (Bijzonder Onderzoeksfonds grant to D.V.D.S.).

* Address correspondence to jean.colcombet@ips2.universite-paris-saclay.fr.

The author responsible for distribution of materials integral to the findings presented in this article in accordance with the policy described in the Instructions for Authors (www.plantphysiol.org) is: Jean Colcombet (jean.colcombet@ips2.universite-paris-saclay.fr).

B.G., H.H., and J.C. designed the research; B.G., J.L., S.B., M.G., F.G., S.P., D.V.D.S., K.H., and J.C. performed research; B.G., J.L., H.H., and J.C. wrote the article.

www.plantphysiol.org/cgi/doi/10.1104/pp.17.00378

 

in some cases. The MAP3K MEKK1 activates the two MAP2Ks MKK1 and MKK2, which converge to activate MPK4 (Ichimura et al., 2006; Nakagami et al., 2006; Gao et al., 2008; Qiu et al., 2008). MPK3 and MPK6 are both activated by MKK4 and MKK5, but their upstream MAP3K(s) have not yet been unambiguously identified (Asai et al., 2002).

Whereas the MKK4/5-MPK3/6 module is thought to positively regulate immunity, the MEKK1-MKK1/2-MPK4 module was first described as a negative regulator (Petersen et al., 2000; Brodersen et al., 2006). Indeed, *mekk1*, *mkk1/mkk2*, and *mpk4* loss-of-function mutants display constitutively activated defense responses in the absence of pathogens, spontaneous cell death, and the accumulation of reactive oxygen species (ROS) and salicylic acid (SA; Petersen et al., 2000; Gao et al., 2008), resulting in growth defects and dwarfed plants (Pitzschke et al., 2009; Frei dit Frey et al., 2014). Their altered developmental phenotypes can be partially suppressed by mutations/transgenes reducing SA levels, such as *sid2* and *NahG*, as well as by growth at high temperature (Brodersen et al., 2006; Su et al., 2007). Recently, two allelic series of loss-of-function mutations able to fully suppress autoimmune-related growth defects of *mekk1*, *mkk1/mkk2*, and *mpk4* were identified in a forward genetic screen (Kong et al., 2012; Zhang et al., 2012). *summ1* (*suppressor of mkk1 mkk2 1*) is mutated in *MEKK2*, the closest homolog of *MEKK1*, and *summ2* is mutated in a nucleotide-binding leucine-rich repeat (NB-LRR) protein. These results suggest that the MEKK1-MKK1/2-MPK4 module is guarded by the NB-LRR protein SUMM2 to avoid its manipulation by pathogen effectors. In accordance with the current model, the MEKK1-MKK1/2-MPK4 module would then be a positive regulator of stress responses.

Despite being activated by stresses with similar kinetics, three iconic MAPKs, MPK3, MPK4, and MPK6, are not functionally fully redundant. A growing number of publications describe MAPK substrates that may be targeted specifically by a single or a combination of several MAPKs (for review, see Bigeard et al., 2015).

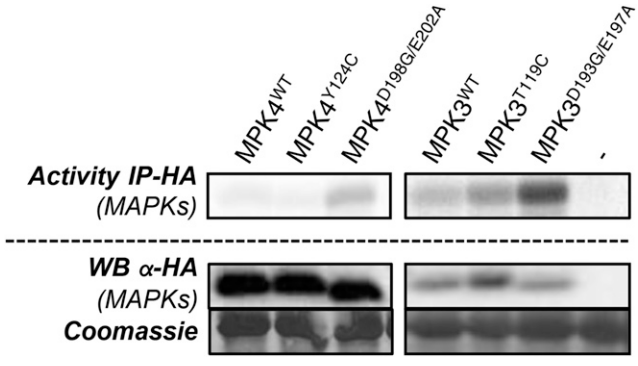


**Figure 1.** Activity of MPK3 and MPK4 wild-type and CA plants expressed in mesophyll protoplasts. The kinase activity shows HA immunoprecipitation (IP) of HA-tagged MAPK (wild type and mutant) expressed in Columbia-0 (Col-0) mesophyll protoplasts. Western blots (WB) show protein levels.

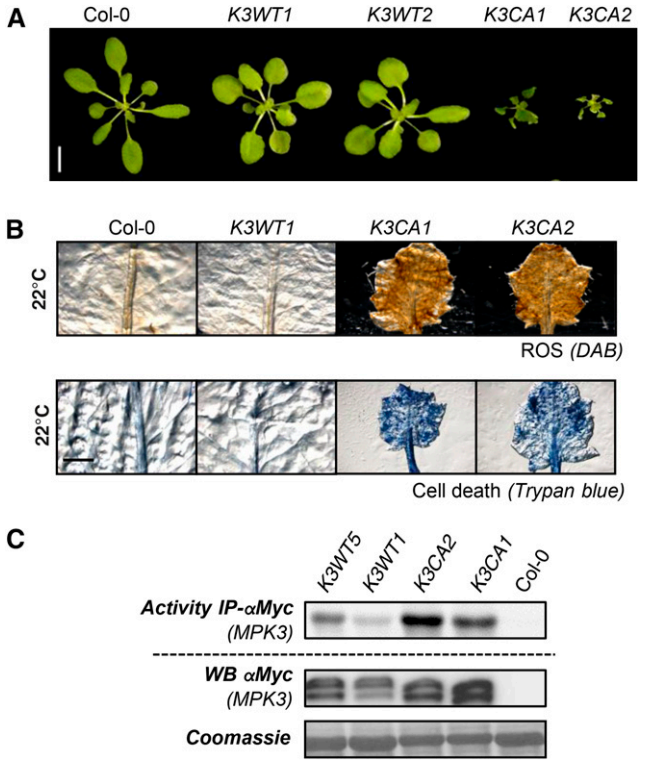


**Figure 2.** Phenotypes of plants expressing c-myc-tagged *K3WT* and *K3CA*. A, Representative photographs of 30-d-old rosettes of the indicated genotypes. Bar = 1 cm. B, Trypan Blue and DAB staining of representative leaves from the indicated genotypes. Bar = 2 mm. C, Kinase activity of MPK3-myc after immunoprecipitation (IP) using anti-c-myc antibody from the indicated genotypes. Western blots (WB) show protein levels.

*mpk3* and *mpk6* single mutants show normal development, whereas *mpk3mpk6* double mutants are barely viable (Wang et al., 2007). This strong developmental redundancy makes the investigation of the stress-related roles of these kinases complicated. The fact that some substrates, such as ACS2/6, ERF6, and WRKY22/28/33, are targeted by both MPK3 and MPK6 indicates that these MAPKs have at least partially similar roles in plant defense regulation (for review, see Bigeard et al., 2015). Interestingly, the phenotypical characterization of single mutants showed specific functions. For example, *mpk3* mutants are susceptible to the necrotrophic pathogen *Botrytis cinerea*, whereas *mpk6* is not (Ren et al., 2008). Both *mpk3* and *mpk6* mutants are impaired in flg22-triggered stomatal closure, suggesting that they have collaborative functions in the regulation of guard cell volume rather than redundant functions (Montillet et al., 2013). *mpk3* but not *mpk6* overproduces RBOHD-dependent ROS burst upon MAMP perception, suggesting an *MPK3*-specific negative role in MAMP-triggered immunity (MTI) responses (Ranf et al., 2011). Recently, an extensive transcriptomic analysis of *mapk* mutants upon flg22 treatment underlined the specificities of each MAPK in gene expression reprogramming during MTI (Frei dit Frey et al., 2014).

Our laboratory reported the identification of mutations that render Arabidopsis MAPKs constitutively active (CA; Berriri et al., 2012). Our previous work focused on plants expressing CA-MPK4 and demonstrated that these point mutations do not alter substrate specificity, making them a powerful tool to provide complementary evidence for loss-of-function-based analysis of MAPKs. In this study, we used the same approach to tackle MPK3 function. Our detailed characterization of *CA-MPK3* lines brings new insights to the role of MPK3 in innate immunity.

## RESULTS

### The Dual Mutation D193G/E197A Results in Constitutive Activation of MPK3

We recently reported the identification of two sets of mutations, Y144C and D218G/E222A, which trigger constitutive autoactivity to recombinant Arabidopsis MPK6 (Berriri et al., 2012). In vitro expression of CA MAPKs suggested that CA mutations may be transferrable to other plant MAPKs but that all mutations do not systematically activate MAPKs in planta. To select for mutations that trigger the strongest in vivo autoactivity in the stress-related MPK3, we expressed human influenza hemagglutinin (HA)-tagged $MPK3^{WT}$, $MPK3^{T119C}$, and $MPK3^{D193G/E197A}$, as well as $MPK4^{WT}$, $MPK4^{Y124C}$, and $MPK4^{D198G/E202A}$ as controls, using the mesophyll protoplast expression system. We assayed MAPK activity after HA immunoprecipitation for their ability to phosphorylate myelin basic protein (MBP) and found that $MPK3^{D193G/E197A}$ and, to a lesser extent, $MPK3^{T119C}$ were more active than $MPK3^{WT}$ (Fig. 1).

### Plants Expressing $MPK3^{D193G/E197A}$ Show Higher MPK3 Activity and Dwarfism Associated with ROS Accumulation and Cell Death

To investigate MPK3 function further, we created Arabidopsis transgenic lines expressing $MPK3^{D193G/E197A}$. For this purpose, the *mpk3-1* knockout mutant was transformed with vectors allowing the expression of the c-myc-tagged genomic sequence of $MPK3^{WT}$ and the mutated version $MPK3^{D193G/E197A}$. These lines will be further referred to as *K3WT* and *K3CA*, respectively. Under standard growth conditions (soil, 22°C, long days), all *K3CA* T1 plants showed a dwarfed morphology

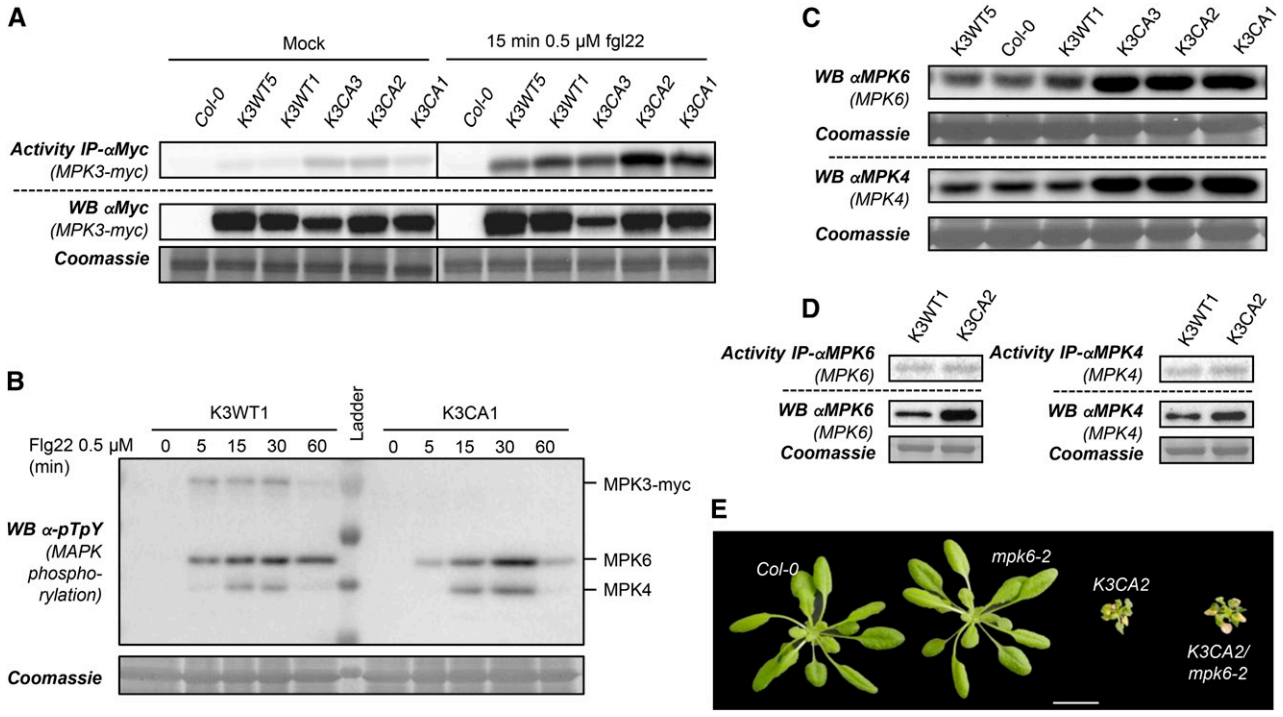


**Figure 3.** Characterization of MAPK protein levels and PAMP-triggered immunity in *K3WT* and *K3CA* lines. A, Kinase activity of MPK3-myc after immunoprecipitation (IP) using anti-c-myc antibody from in vitro plantlets of the indicated genotypes treated with flg22 for 15 min. Western blots (WB) show protein expression levels. B, Kinase phosphorylation in the MAPK activation loop monitored by western blot using anti-pTpY antibody from *K3WT1* and *K3CA1* transgenic lines treated with 1 $\mu$M flg22 for the indicated times. Note that the anti-pTpY antibody does not detect the phosphorylated MPK3 activation loop when it is mutated (D193G/E197A). C, Western blot analyses of MPK4/6 levels using MAPK-specific antibodies in rosettes of pot-grown plants of the indicated backgrounds. D, Kinase activity of MPK4 and MPK6 after immunoprecipitation using specific antibody from rosettes of the indicated genotypes. Western blots show protein expression levels. E, Representative photographs of 1-month-old *K3CA2/mpk6-2* plants compared with parental lines and Col-0. Plants were cultivated at 22°C on soil in a culture chamber. Bar = 2 cm.

associated with leaf serration and reduced fertility, whereas *K3WT* T1 plants did not show any noticeable morphological phenotype when compared with Col-0 ($n > 20$ for both genotypes). This phenotype was maintained in homozygous lines carrying a single insertion (Fig. 2A). Trypan Blue and 3,3′-diaminobenzidine (DAB) staining showed that this dwarfism is associated with spontaneous cell death and constitutive ROS accumulation (Fig. 2B). To characterize MPK3 protein levels in the different genetic backgrounds, we performed western-blot analysis of 15-d-old plantlets grown in vitro (Supplemental Fig. S1A). Unluckily, MPK3 antibody, which is raised against the 11 C-terminal residues of MPK3, does not detect the C-terminally c-myc-tagged MPK3 fusion proteins, making the comparison of MPK3 protein level between Col-0 and transgenic lines unachievable. Western immunoblots using c-myc antibodies showed that the level of MPK3-myc varies from one transgenic line to another, as expected when T-DNA insertion occurs randomly in the genome. As an alternative to direct MPK3 protein detection, we performed reverse transcription-quantitative PCR (RT-qPCR) analyses and found that the level of expression of *MPK3-myc* transcripts in transgenic lines, which also varies from one line to another, is overall similar to the level of *MPK3* transcripts in Col-0 (Supplemental Fig. S1B). c-myc-based immunoprecipitation from *K3WT* and *K3CA* plantlets grown in vitro followed by kinase assays showed that *K3CA* lines exhibit a higher MPK3 activity than *K3WT* lines (Supplemental Fig. S1C). Similar results were obtained when the c-myc-based immunoprecipitation was performed from rosettes of pot-grown plants showing the strong dwarf phenotype (Fig. 2C). Importantly, the MPK3 kinase activities, as well as the dwarf phenotype of the *K3CA* plants, were specific for the CA mutation and apparently independent of MPK3 protein abundance levels (Fig. 2; Supplemental Fig. S1). Remarkably, *K3CA* plantlets grown in vitro showed no obvious phenotype while pot-grown plants showed a dwarfed morphology, suggesting that, in addition to the constitutive MPK3 activity, environmental factors are required for its full establishment.

### K3CA Plants Still Respond to flg22 and Do Not Affect MPK4/6 Activities

To determine whether the constitutive activity of *K3CA* plants interferes with MTI signaling, we challenged in vitro seedlings with the model MAMP flg22. As shown in Figure 3A, MPK3 activities in *K3CA* lines still increased drastically in response to flg22 compared with *K3WT* lines, demonstrating that the constitutive activity of MPK3 does not lead to a desensitized MPK3 pathway. It also indicates that the MPK3 activity increase triggered by CA mutations is mild compared with the MPK3 activity after MAMP treatment and that CA mutations, which are located in the activation loop close to the TEY activation motif, do not affect its phosphorylation by upstream MAP2Ks. As cross talk and compensatory mechanisms between MTI-related MAPK modules exist (Frei dit Frey et al., 2014), we were curious to see whether the constitutive activity of MPK3 might provoke changes in MPK6 and MPK4 activation. For this purpose, we used western

**A**

| Enriched GO terms | Pvalue (Bonferroni) | Fold Enrichment |
|---|---|---|
| defense response | $1{,}0.10^{-30}$ | 2,5 |
| immune response | $5{,}5.10^{-30}$ | 4,2 |
| cell death | $1{,}0.10^{-17}$ | 3,6 |
| response to bacterium | $6{,}2.10^{-11}$ | 3,1 |
| response to fungus | $1{,}3.10^{-02}$ | 1,8 |
| response to salicylic acid stimulus | $5{,}5.10^{-08}$ | 3,4 |
| response to ethylene stimulus | $3{,}6.10^{-02}$ | 2,1 |
| response to oxidative stress | $4{,}7.10^{-06}$ | 2,4 |
| callose deposition during defense response | $2{,}4.10^{-02}$ | 6,7 |
| indole derivative metabolic process | $3{,}1.10^{-07}$ | 6,1 |

**B**

| Enriched GO terms | Pvalue (Bonferroni) | Fold Enrichment |
|---|---|---|
| response to endogenous stimulus | $1{,}3.10^{-10}$ | 2,1 |
| photosynthesis | $1{,}3.10^{-08}$ | 3,8 |
| response to jasmonic acid stimulus | $3{,}6.10^{-03}$ | 3,0 |
| response to auxin stimulus | $6{,}3.10^{-03}$ | 2,2 |
| oxidation reduction | $2{,}4.10^{-04}$ | 1,7 |
| secondary metabolic process | $9{,}4.10^{-04}$ | 2,1 |
| starch biosynthetic process | $1{,}2.10^{-03}$ | 9,8 |
| cell wall organization | $7{,}1.10^{-03}$ | 2,3 |

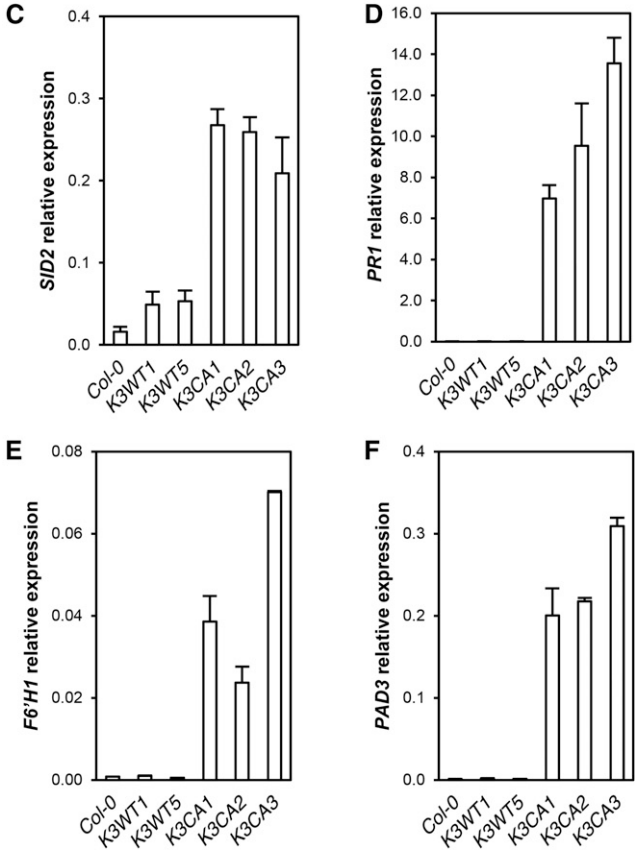


**Figure 4.** Misregulated genes in *K3CA* lines. A, Top enriched GO terms among the up-regulated genes. B, Top enriched GO terms among the down-regulated genes. C to F, *SID2*, *PR1*, *F6′H1*, and *PAD3* transcript levels in *K3CA* and *K3WT* lines. Data are means ± SD of three technical repetitions.

immunoblots to monitor flg22-dependent activation loop phosphorylation of MPK4 and MPK6 in representative *K3WT* and *K3CA* lines (Fig. 3B). We did not observe any differences between these lines, as MPK4 and MPK6 had the typical kinetics of phosphorylation, with a rapid increase, a plateau at 15 to 30 min, and a decrease after 1 h (Fig. 3B). MPK4 and MPK6 protein levels also were not affected in in vitro-grown plantlets of *K3CA* lines compared with Col-0 and *K3WT* lines (Supplemental Fig. S1A). On the other hand, in the case of dwarfed plants grown on soil, we monitored an increase in the amount of MPK4/6 proteins in *K3CA* lines compared with Col-0 and *K3WT* lines (Fig. 3C). To exclude that *K3CA* dwarfism could be due to a higher accumulation of MPK4/6, which would trigger stronger MPK4/6 activities, we measured their activity after immunoprecipitation but did not see any increases in the *K3CA* line (Fig. 3D). Finally, we crossed *K3CA2* plants with *mpk6-2* but found that a lack of *MPK6* does not suppress *K3CA* dwarfism (Fig. 3E). These results suggest that MPK6 likely does not mediate *K3CA* dwarfism.

### K3CA Lines Show Induction of Stress-Related Genes

In order to identify the genes misregulated in *K3CA* lines, we performed a global transcriptome analysis. Plants of *K3CA* and *K3WT* lines, three independent lines for each, were grown on soil for 30 d. RNA was extracted and hybridization was performed on microarrays according to an experimental design limiting the positional effect of T-DNA insertions (Supplemental Fig. S2). A total of 1,848 up-regulated and 1,483 down-regulated CATMA probes, corresponding to 1,769 and 1,436 unique genes, were found in *K3CA* lines compared with *K3WT* lines, respectively (adjusted with a false discovery rate $P < 0.05$; Supplemental Tables S1 and S2). To identify the physiological processes that are altered in *K3CA* lines, we performed a Gene Ontology (GO) analysis of the differentially expressed genes. Notably, the set of up-regulated genes showed a significant enrichment of GO categories related to responses to pathogens, defense and immunity, and cell death as well as responses to oxidative stress and to the stress-related hormones ethylene and SA (Fig. 4A; Supplemental Table S3). Among the down-regulated genes, we found an enrichment in the categories of metabolism (photosynthesis, starch, and secondary metabolism) as well as the hormones auxin and jasmonic acid (Fig. 4B; Supplemental Table S3). The transcriptomic data obtained were confirmed by RT-qPCR using a set of relevant genes. Notably, the defense-related genes *SID2* (*SALICYLIC ACID INDUCTION-DEFICIENT2*), *PR1* (*PATHOGENESIS-RELATED GENE1*), *PAD3* (*PHYTOALEXIN DEFICIENT3*), and *F6′H1* (*FERULOYL-COA 6′-HYDROXYLASE1*) were all up-regulated in *K3CA* lines (Fig. 4, C–F). Comparing our transcriptomic data with previously published ones revealed that about 40% and 30% of the genes up-regulated upon MAMP perception (30-min flg22 treatment) and bacterial infection (2 h post *Pseudomonas syringae* inoculation), respectively, were also up-regulated in *K3CA* lines (Supplemental Fig. S3, A–E). This result indicates that *K3CA* lines display active defenses due to MPK3 activation. It also suggests that MPK3 activity is important for the transcriptional reprograming during the first steps of pathogen perception.

### K3CA Plants Produce Ethylene and Accumulate SA, Camalexin, and Scopoletin

To understand the extent to which the transcriptomic data translate into a physiological phenotype, we quantified the levels of some defense-related hormones in *K3CA* plants. Ethylene production by 1-aminocyclopropane-1-carboxylic acid synthases (ACS) was reported to be up-regulated by the expression of a *Nicotiana tabacum* CA MEK2, which activates MPK3 and MPK6 (Liu and Zhang, 2004). Ethylene measurements were carried out using a photoacoustic detector. Surprisingly, it revealed only a minor increase of ethylene production in *K3CA* compared with *K3WT* lines (Supplemental Fig. S4A). In contrast, we found that total and free SA accumulated 10 to 20 and 2 to 3 times, respectively, in *K3CA* compared with *K3WT* and Col-0 plants (Fig. 5, A and B). Finally, camalexin and scopoletin, two major phytoalexins, were about 160 and 7 times more abundant, respectively, in *K3CA* than in *K3WT* and Col-0 plants (Fig. 5, C and D). Altogether, these findings established that MPK3 activity results in altered accumulation of defense compounds like defense hormones and phytoalexins.

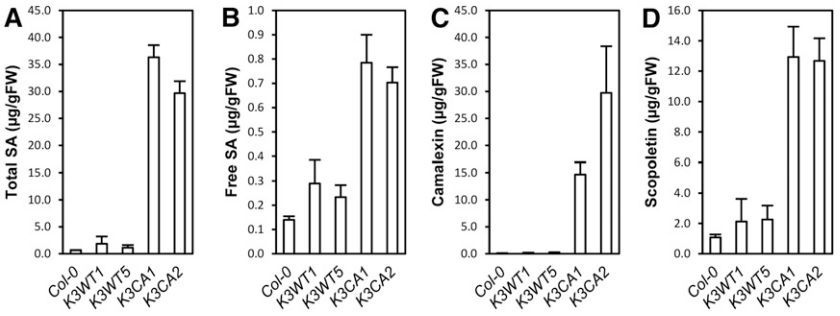


**Figure 5.** Characterization of SA and phytoalexin contents in *K3CA* lines. Total SA (A), free SA (B), camalexin (C), and scopoletin (D) contents were measured by HPLC in the indicated lines. Average contents of four independent biological replicates are represented. Error bars show SE. FW, Fresh weight.

### K3CA Phenotypes Are Mostly Dependent of SA Signaling But Independent of Ethylene Signaling

To further investigate the role of MPK3 in ethylene and SA production and the extent to which they contribute to *K3CA* phenotypes, we crossed *K3CA1* plants with the *ein2-50* (*ethylene insensitive2*) mutant impaired in ethylene-mediated signaling (Xu et al., 2008) and with *sid2-2*, a mutant impaired in SA accumulation during pathogen infection (Nawrath and Métraux, 1999). We did not observe any suppression of *K3CA* dwarfism by *ein2-50* (Supplemental Fig. S4B), meaning that ethylene signaling is not of major importance for establishing the *K3CA* phenotype. In contrast, *sid2-2* abolished SA accumulation in *K3CA* plants (Fig. 6, A and B) and led to a partial reversion of the dwarfed phenotype (Fig. 6C). Although *K3CA1/sid2-2* plants were 3 to 5 times bigger than *K3CA1* plants, they still remained affected in their development. In line with this observation, spontaneous ROS accumulation and cell death in *K3CA1* also were only partially suppressed by *sid2-2* (Fig. 6D), as was the up-regulation of *PR1*, which dropped about 100 times in *K3CA/sid2* compared with *K3CA* but still remained severalfold higher compared with Col-0 (Fig. 6E). Additionally, although the decrease of *PAD3* expression in *K3CA/sid2* compared with *K3CA* correlated with the decrease in camalexin contents, the decrease of *F6'H1* apparently had no effect on the level of scopoletin (Fig. 7). These results indicate that scopoletin accumulation, unlike camalexin, is SA independent. Interestingly, the partial suppression of the *K3CA* phenotypes in *K3CA1/sid2-2* plants correlated with the mild decrease in MPK3 activity (Fig. 6F), suggesting that sustainable MPK3 activity is ensured by a positive feedback loop involving SA. Overall, our results show that MPK3 function in plant immunity is dependent on SA signaling.

### Comparison of K3CA and *mpk4* Phenotypes Shows That the Two Mutants Are Closely Related

The similarity in the dwarf, cell death, and enhanced SA level phenotypes of the autoimmune *mpk4* mutant and the *K3CA* lines prompted us to characterize these lines in close detail. The *mpk4* phenotype is similarly related to high levels of the defense hormone SA and is suppressed by growth under high temperature. We grew *K3CA* plants at 28°C and observed an identical suppression of the autoimmune features (Supplemental Fig. S5, A and B). A comparison of the transcriptomes between *K3CA* lines grown on soil and *mpk4* seedlings grown in vitro (Frei dit Frey et al., 2014) revealed 35% and 10% overlaps among the up- and down-regulated genes, respectively (Supplemental Fig. S3B). Interestingly, besides SA, *mpk4* accumulates both scopoletin and camalexin (Fig. 8, A–D). To obtain an overview of the metabolic changes, we performed gas chromatography/mass spectrometry-time of flight profiling of Col-0, *K3CA*, *K3WT*, and *mpk4* plants. We also included the *mips1* mutant, which was shown previously to have

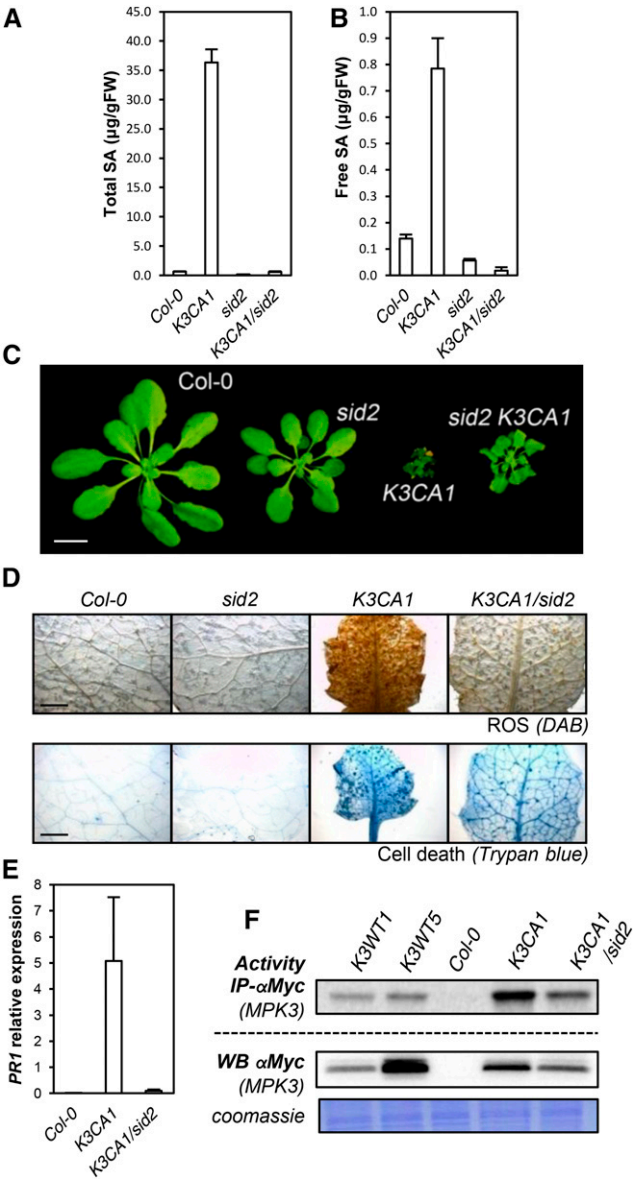


**Figure 6.** SA-related phenotypes of *K3CA* lines. A and B, Total (A) and free (B) SA contents measured by HPLC in the indicated genetic backgrounds. Data are means ± SD of four biological repetitions. FW, Fresh weight. C, Representative photographs of 1-month-old *K3CA1/sid2-2* plants compared with parental lines and Col-0. Plants were cultivated at 22°C on soil in a culture chamber. Bar = 1 cm. D, Representative photographs of *K3CA1/sid2-2* leaves compared with parental lines and Col-0 stained with DAB and Trypan Blue to visualize ROS and cell death. Bars = 2 mm. E, *PR1* transcript levels in the indicated backgrounds. Data are means ± SD of four biological repetitions. F, Kinase activity toward MBP of MPK3-myc immunoprecipitated (IP) from the indicated lines. Western blots (WB) show MPK3-myc levels.

a SA-related autoimmune phenotype (Meng et al., 2009). Overall, 99 peaks were identified corresponding to 91 metabolites (Supplemental Table S4). *K3CA* lines showed 26 and 11 metabolites to be significantly increased and reduced, respectively, compared with *K3WT* ($P < 0.05$). A more careful look to these metabolites

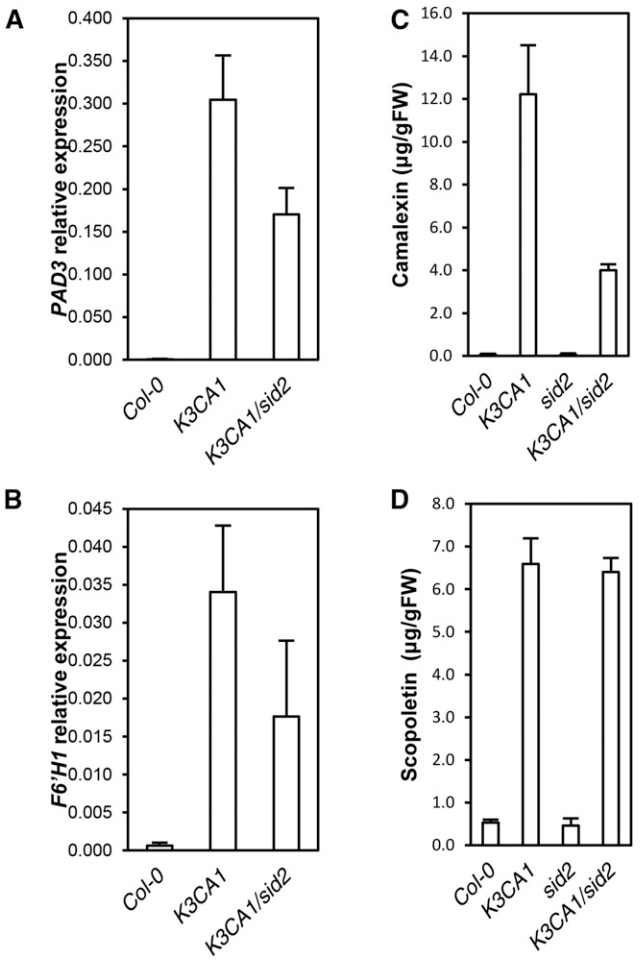


**Figure 7.** SA-related phytoalexin phenotypes of *K3CA* lines. A and B, *PAD3* (A) and *F6'H1* (B) transcript levels in the indicated backgrounds. Data are means ± SD of four biological repetitions. C and D, Camalexin (C) and scopoletin (D) contents measured by HPLC in the indicated genetic backgrounds. Data are means ± SD of four biological repetitions.

showed that 11 amino acids and several molecules of the Krebs cycle, including citric acid, α-ketoglutaric acid, and malic acid, accumulated in *K3CA* plants. Among the reduced metabolites, there were important sugars, such as Glc and Fru, as well as spermidine. Interestingly, we observed a significant correlation between metabolite contents in *K3CA* and *mpk4*, which is another confirmation of the similarities of the responses activated in these two mutant lines (Fig. 8). No correlation was found between *K3CA* and *mips1* (Supplemental Fig. S6), suggesting that the metabolome changes in these autoimmune mutants are not due to the high SA levels and that *K3CA* plants are phenotypically more similar to *mpk4* than to *mips1* plants.

### Mutations That Suppress *mpk4* Are Modifiers of the K3CA Phenotype

Several mutations have been reported to fully suppress *mpk4* dwarfism (Kong et al., 2012; Zhang et al., 2012). In order to test whether these mutations also could suppress *K3CA* dwarfism, we crossed *K3CA2* with *summ1-1* and *summ2-8*. Both *K3CA2/summ1-1* and *K3CA2/summ2-8* were 2 to 3 times bigger than *K3CA2* plants but still much smaller than control plants (*K3WT* and Col-0; Fig. 9A). Cell death and ROS accumulation were partially reduced in *K3CA2/summ2-8* and *K3CA2/summ1-1* (Fig. 9B). Whereas total SA levels also were partially reduced, free SA accumulation was not impacted by the *summ1* or *summ2* mutation (Fig. 9, C and D). Consistently, the transcript levels of the *PR1* gene, which is a marker of SA signaling, were not significantly affected in *K3CA2/summ1* and *K3CA2/summ2* compared with control lines (Supplemental Fig. S7). In contrast, camalexin and scopoletin levels were both reduced in *K3CA2/summ1-1* and *K3CA2/summ2-8* compared with *K3CA2*, with a stronger reduction in camalexin, as were the biosynthetic marker genes of

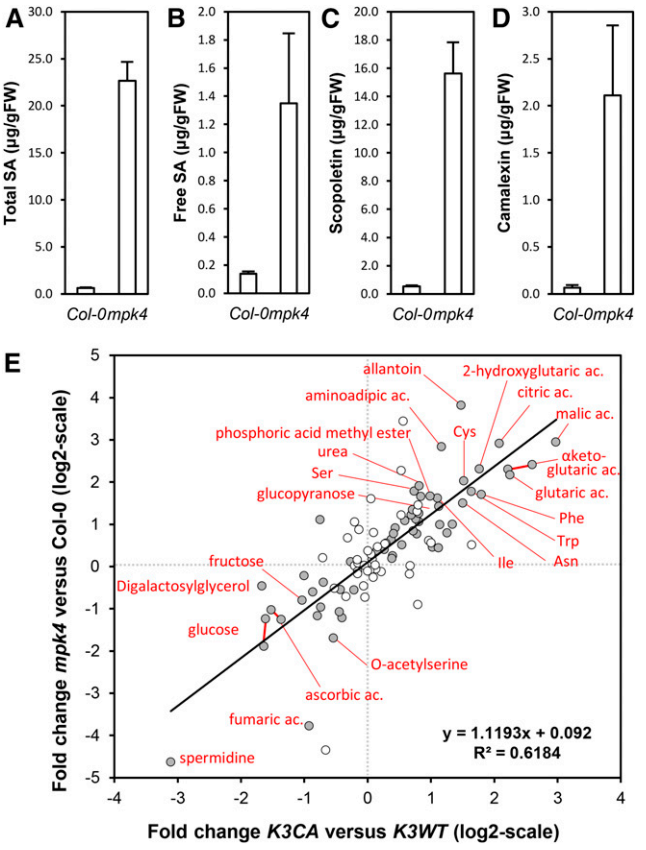


**Figure 8.** Comparison of metabolite contents of *mpk4* versus *K3CA* plants. A to D, Total SA (A), free SA (B), scopoletin (C), and camalexin (D) contents of *mpk4* measured by HPLC. Data are means ± SD of four biological repetitions. FW, Fresh weight. E, Metabolite analysis of *K3CA* and *mpk4* plants. Means of fold changes ($\log_2$) of *K3CA*/*K3WT* (*x* axis) are plotted against means of fold changes ($\log_2$) of *mpk4*/Col-0 (*y* axis). Gray dots show metabolites that are significantly misaccumulated in *K3CA* plants (Wilcoxon, Mann-Whitney test with $P < 0.05$). For clarity, compound names are indicated for fold changes ($\log_2$) higher than 1.5 or lower than −1.5.

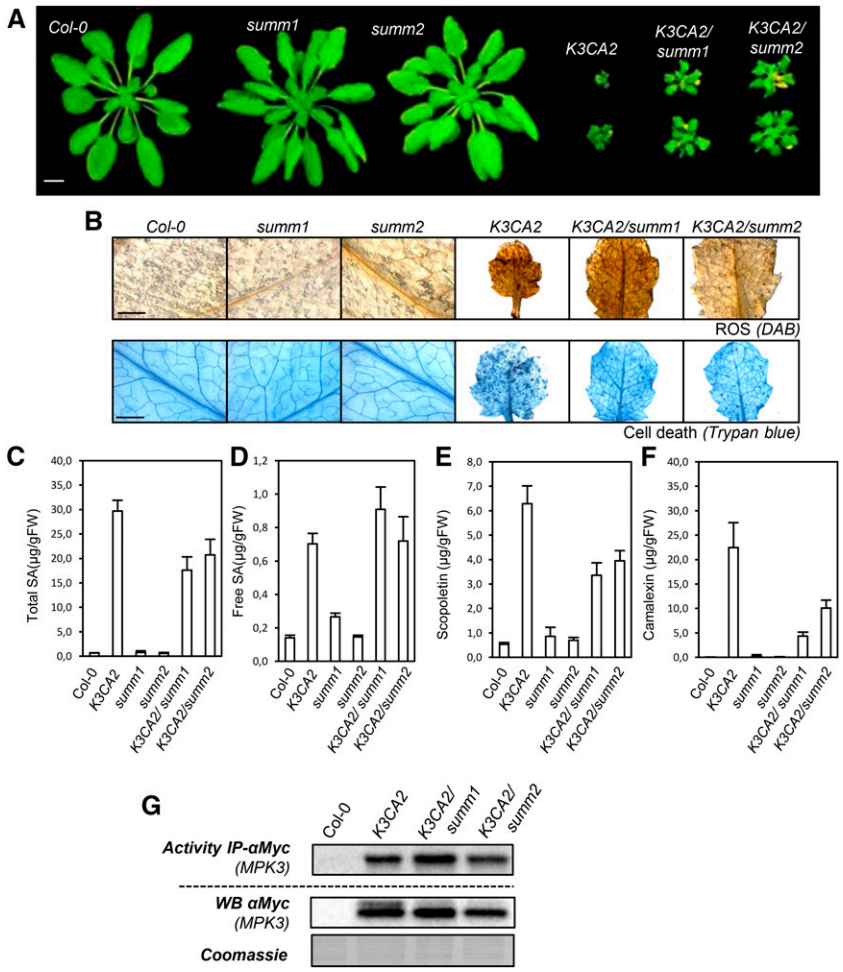


**Figure 9.** Phenotypes of *K3CA2* crossed with *summ* mutants. A, Representative photographs of *K3CA2/summ1-1* and *K3CA2/summ2-8* plants compared with parental lines and Col-0. Plants were cultivated at 22°C on soil in a culture chamber. Bar = 1 cm. B, Representative photographs of *K3CA-2/summ1-1 and K3CA-2/summ2-8* leaves compared with parental lines and Col-0 stained with DAB and Trypan Blue to visualize ROS and cell death. Bars = 2 mm. C to F, Free (C) and total (D) SA, scopoletin (E), and camalexin (F) contents measured by HPLC in the indicated genetic backgrounds. Data are means ± SD of four biological repetitions. FW, Fresh weight. G, Kinase activity of MPK3-myc immunoprecipitated (IP) from the indicated genetic background. Western blots (WB) show protein expression levels.

these pathways (Fig. 9, E and F; Supplemental Fig. S7). Besides, unlike what was observed in *K3CA/sid2*, the partial suppression of the *K3CA* phenotypes in *K3CA1/summ1* and *K3CA/summ2* plants did not appear to be linked to a decrease in MPK3 kinase activity or protein level (Fig. 9G). Altogether, these results indicate a bifurcation of the innate immunity pathway at the level of MPK3 for scopoletin and camalexin biosynthesis on the one hand and the MPK4-dependent SUMM1 and SUMM2 regulation on the other hand.

## DISCUSSION

MAPKs play central roles in MTI (Bigeard et al., 2015). Recent data suggest that they also have an important function during effector-triggered immunity (ETI; Tsuda et al., 2013). The main difference between these two processes lies in their kinetics of activation. MPK3 and MPK6 are rapidly and transiently activated upon MAMP perception, whereas this activation takes longer and is sustained for hours after the detection of a pathogenic effector (Tsuda et al., 2013). MPK4 also is activated transiently by MAMPs, but only indirect data suggest its activation during ETI (Berriri et al., 2012). These data fit the idea that MTI and ETI correspond to similar responses, differing mainly by their temporal pattern and amplitude of activation. The identification of particular roles of the MAPKs in the context of MTI and ETI is complex. A widely used strategy consists of using loss-of-function or gain-of-function protein kinase mutants. The gain-of-function strategy has been used extensively to investigate the role of MAP2Ks, for which replacing the two phosphorylated residues in the activation loop by phospho-mimicking residues usually triggers constitutive activity. We recently applied a gain-of-function strategy to the MAPK level by identifying mutations triggering constitutive activation (Berriri et al., 2012). As an alternative to inducible lines, which result in high protein accumulation and, thereby, possible nonspecific events, we created Arabidopsis lines expressing CA MAPKs under the control of their native promoter using genomic loci.

### Plants Expressing CA-MPK3 Show Up-Regulation of SA-Dependent and Independent Defense Responses

Plants expressing CA-MPK3 showed autoimmune phenotypes characterized by dwarfism associated with spontaneous cell death, accumulations of ROS and SA,

and modification of metabolism to produce the phytoalexins scopoletin and camalexin. MPK3 and MPK6 are thought to play redundant roles during immunity, as they share several features, notably their kinetics of activation and some of their substrates. For this purpose, it would have been interesting to compare the phenotypes of *K3CA* and *K6CA* plants. However, so far, we have been unable to create lines expressing CA-MPK6, possibly because, in our case, a constitutive activation of MPK6 in planta is deleterious. The enhanced production of camalexin by CA-MPK3 plants agrees with the findings that, upon *B. cinerea* infection, MPK3 and MPK6 have been proposed to phosphorylate the transcription factor WRKY33, which binds camalexin biosynthetic gene promoters and triggers camalexin accumulation (Ren et al., 2008; Mao et al., 2011). Moreover, our work confirms the report that Arabidopsis plants expressing dexamethasone-inducible CA-MKK5$^{DD}$ or *Nt*MEK2$^{DD}$, MAP2Ks upstream of MPK3 and MPK6, accumulate intermediate levels of camalexin (Ren et al., 2008; Lassowskat et al., 2014). We also found that CA-MPK3 is able to induce the accumulation of the phytoalexin scopoletin, which is known to have a role in defense in tobacco (Chong et al., 2002) and in iron uptake in Arabidopsis (Schmidt et al., 2014). *K3CA* plants accumulate intermediate compounds of the Krebs cycle, such as citric, malic, and α-ketoglutaric acids, suggesting an enhanced turnover of the tricarboxylic acid cycle. In agreement, sugars such as Glc and Fru were underaccumulated in *K3CA* lines. We also noticed a significant increase in several amino acids, which could be the consequence of cell death-related protein degradation.

*K3CA* plants produce slightly more ethylene than wild-type plants. However, *ein2* was unable to suppress the *K3CA* dwarf phenotype, suggesting that ethylene is not a major player in MPK3 responses. This contradicts data reporting that ethylene is an important actor in the MKK5-dependent cell death (Liu et al., 2008) and the fact that ACS2/6 are MPK3/6 substrates (Liu and Zhang, 2004; Han et al., 2010). Although these contrasting results may depend on the use of different experimental systems, different outcomes also may stem from different expression and activation levels. In our work, MPK3 was expressed at endogenous levels and moderately activated by CA mutations. In contrast to ethylene, *K3CA* plants strongly accumulated SA, and consistently, mutation of the *SID2* gene partially suppressed the morphological defects in CA-MPK3 plants, such as ROS accumulation and cell death. SA overaccumulation often is observed in autoimmune mutants and, therefore, is believed to be a crucial factor for inducing cell death (Bruggeman et al., 2015), as most of the mutant phenotypes are indeed suppressed by inhibiting SA biosynthesis. For example, the cell death phenotypes of *mpk4* and *mips1* are suppressed by the expression of the bacterial SA hydrolase *nahG* or by the introgression of a *sid2* mutation (Brodersen et al., 2006; Meng et al., 2009). Nevertheless, not all MPK3 functions depend on *SID2*-triggered SA accumulation. First, while totally abolishing SA accumulation, *sid2* did not fully revert *K3CA*-dependent dwarfism. Additionally, only camalexin accumulation was partially reduced by *sid2*, whereas scopoletin was unchanged. SA-dependent genes, such as *PR1*, which are highly expressed in *K3CA* lines, are only partially reduced by *sid2*. This result is in agreement with other studies. For example, cytokinin treatment induces scopoletin synthesis independently of SA (Grosskinsky et al., 2011), and the auxin 2,4-D but not SA or methyl jasmonate treatment triggered scopoletin synthesis in Arabidopsis (Kai et al., 2006). In line with a previous report (Tsuda et al., 2013), this result also illustrates the robustness and complexity of the defense signaling pathways modulated by a sustained activity of MPK3 that is both SA dependent and independent.

### Plants Expressing CA-MPK3 Phenocopy Loss-of-Function Mutants of the MEKK1-MKK1/2-MPK4 Pathway

Overall, the *K3CA* phenotype strongly resembles to loss-of-function mutants of the MEKK1-MKK1/2-MPK4 module (Petersen et al., 2000; Ichimura et al., 2006; Nakagami et al., 2006; Gao et al., 2008; Qiu et al., 2008). Like *mpk4* plants (Brodersen et al., 2006), *K3CA* lines accumulated SA, camalexin, and scopoletin as well as ROS, but not to the same extent. Both *K3CA* and *mpk4* show spontaneous cell death and comparable transcriptomes and metabolomes. On the other hand, the SA-dependent cell death phenotype of *mips1* (Meng et al.,

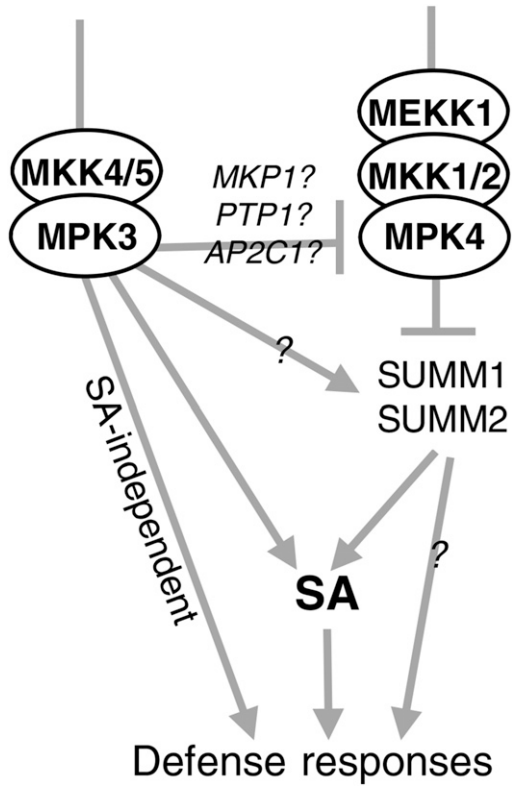


**Figure 10.** Working model for MPK3 function.

2009) was not correlated with a similar metabolome, as found for *mpk4* and *K3CA* lines. Altogether, these data indicate the specificity of the MAPK immune phenotype and how constitutive activation of MPK3 alone results in the deregulation of similar aspects of defense as mutations in the MEKK1-MKK1/2-MPK4 module.

The phenotype of mutants impaired in the MEKK1-MKK1/2-MPK4 module has been attributed to the activation of a guarding pathway containing SUMM1/MEKK2 and SUMM2 (Kong et al., 2012; Zhang et al., 2012). Consequently, mutations impairing one of these two genes fully suppress *mpk4* dwarfism as well as SA accumulation and the deregulation of defense marker genes (Kong et al., 2012; Zhang et al., 2012). The SUMM1/2 module was introgressed into *K3CA* plants to investigate whether it also regulates MPK3-related functions. The *K3CA* dwarfism, metabolite and ROS accumulation, as well as cell death phenotypes were partially reverted, but not to the same extent as in the *summ1* and *summ2* crosses with *mpk4*. This suggests that MPK3 regulates stress responses both dependently and independently of SUMM1/2 (Fig. 10). Our group recently showed that MPK3 also functions to restrict MAPK activation during MAMP signaling (Frei dit Frey et al., 2014). Indeed, in *mpk3* plants, flg22-triggered MPK4 and MPK6 activation lasts longer than in wild-type plants. A possible mechanism is provided by various MAPK-triggered phosphatases that act on the immune MAPKs in a negative feedback loop. MAP Kinase Phosphatase1 (MKP1), Protein Tyr Phosphatase1, and AP2C1 all have been shown to reduce stress-triggered MAPK activation (Schweighofer et al., 2007; Bartels et al., 2009; Anderson et al., 2011). MKP1 itself is actually phosphorylated by MPK6, suggesting that it functions in negatively regulating MAPK kinetics during MAMP perception (Park et al., 2011). Therefore, it is possible that, in *K3CA* plants, the reduced basal activity of MPK4 is sufficient to trigger the activation of the guarding module SUMM1/2 and, thereby, leads to an autoimmune phenotype similar to that of *mpk4*. This could account for the partial reversion of the *K3CA* phenotype by *summ1* and *summ2*. It is also plausible that MPK3 directly activates the SUMM1/2 module. Indeed, we observed an up-regulation of *SUMM1* in *K3CA* plants that might be independent of MPK4 function. The fact that *summ1* and *summ2* do not fully suppress the *K3CA* phenotype also suggests that not all MPK3 responses depend on *SUMM1/2*. For example, the accumulation of camalexin and scopoletin is poorly suppressed by *summ1/2* mutations in the *K3CA* lines. Since these two phytoalexins also accumulate in *mpk4*, it would be informative to know the extent to which their accumulation is suppressed in *mpk4* by the *summ1/2* mutations. Interestingly, SUMM2, an R gene of the CC-NB-LRR family, most likely triggers an NDR1-dependent signaling cascade leading to ETI (Aarts et al., 1998). It would be interesting to examine whether the *K3CA* phenotype also is suppressed by *ndr1* and, thus, genetically define how the signaling cascades are connected. Furthermore, MPK3/6 kinases also have been unambiguously shown to be activated during the perception of the *Xanthomonas* effector AvrRPT2 by its cognate TIR-NB-LRR-type receptor RPS2 (Tsuda et al., 2013). One possibility is that the *SUMM1/SUMM2*-independent part of *K3CA* corresponds to the MPK3 function in ETI signaling. Overall, our study provides new insights into MAPK signaling in innate immunity but also raises a number of new questions that require future studies in this field.

## MATERIALS AND METHODS

### Genetic Material and Growth Conditions

The *Arabidopsis thaliana* wild-type ecotype Col-0, *mpk3-1* (Wang et al., 2007), *mpk4-2* (Nakagami et al., 2006), *mips1* (Meng et al., 2009), *sid2-2* (Nawrath and Métraux, 1999), and *summ2-8* and *summ1-1* (Kong et al., 2012; Zhang et al., 2012) were used in this study.

To generate transgenic lines expressing CA-MPK3, two 3,056- and 723-bp PCR products, corresponding to *MPK3* loci upstream and downstream of the stop codon, were amplified using the iProof (Bio-Rad) polymerase and Pr0112/Pr0113 and Pr0114/Pr0115 sets of primers (Supplemental Table S5) from Col-0 genomic DNA. Fragments were cloned in *pGEMTeasy* following the manufacturer's protocol (Promega) and fully sequenced. The *MPK3* locus was then reassembled in *pGREEN0229* (Hellens et al., 2000) using appropriate restriction enzymes to create *pGREEN-MPK3$^{wt}$*. A PCR fragment containing the PC2 tag (Bigeard et al., 2014) was then amplified using Pr0159/Pr0160 primers, digested with *Bgl*II, and inserted in the unique compatible *Bam*HI site of *pGREEN-MPK3$^{wt}$* to create *pGREEN-MPK3$^{wt}$-PC2*. Finally, point mutations were created as described previously using Pr0317/Pr0318 primers to create the *pMPK3::MPK3$^{D193G/E197A}$-PC2* vector (Berriri et al., 2012). Whole constructs were sequenced before *Agrobacterium tumefaciens* transformation. *mpk3-1* was then transformed by floral dipping (Clough and Bent, 1998). Positive transformants were selected on glufosinate. Based on the segregation of glufosinate resistance, lines carrying a single insertion were first selected and, in the next generation, plants carrying a homozygous T-DNA insertion were identified. With the exception of *K3WT* and *K3CA* transgenic lines and crosses, which were generated in a greenhouse, all described experiments were performed using plants grown in a growth cabinet (Percival) in long-day conditions, with a humidity of 70% at 22°C, if not mentioned otherwise.

### Kinase Assay and Western Blot from Plants

For the protoplast experiment, appropriate wild-type and mutant open reading frames (*MPK3*, *MPK3$^{T119C}$*, *MPK3$^{D193G/E197A}$*, *MPK4$^{WT}$*, *MPK4$^{Y124C}$*, and *MPK4$^{D198G/E202A}$*) in pDNR207 were recombined in pHaGWF7 using LR enzyme mix following the manufacturer's protocol (Invitrogen). Protoplasts were prepared from Col-0 leaves and transformed following published protocols (Yoo et al., 2007).

Kinase assays and western-blot analyses were performed as described previously (Berriri et al., 2012). Briefly, for kinase assays, proteins were extracted in a nondenaturant buffer and normalized to 1 $\mu$g $\mu$L$^{-1}$ using Bradford reagent. A total of 100 $\mu$g was then used for the immunoprecipitation/kinase assay on MBP and 20 $\mu$g for related western blots. In the figures 1, 2, 3, 6, and 9, the top image shows the radioactive labeling of MBP and the bottom one shows the blot demonstrating protein concentrations and its cognate Coomassie Blue staining of the membrane at the level of the large subunit of Rubisco. If samples were used only for western blots, proteins were extracted using Laemmli 2× buffer (v/w), and 10 $\mu$L was loaded on SDS gels.

### DAB and Trypan Blue Staining

ROS staining was performed as described previously (Daudi and O'Brien, 2012). For Trypan Blue staining, plant leaves were boiled 1 min in Trypan Blue solution (3.3 mg mL$^{-1}$ Trypan Blue, 33.3% acetic acid, 33.3% phenol, and 33.3% glycerol) diluted in 1 volume of 100% ethanol. Leaves were then bleached in choral hydrate (2.5 g mL$^{-1}$) and conserved in 50% glycerol. Photographs were taken using a binocular loop Leica MZ16F apparatus.

### Transcriptome and qPCR Experiments

The transcriptomic experiment was performed in Transcriptome Platform following an established protocol (Danquah et al., 2015). Rosettes of 1-month-old

plants grown in Percival were collected. RNAs were extracted using the NucleoSpin RNA kit (Macherey-Nagel). cRNA were synthesized, labeled, and hybridized on CATMAv7 Agilent arrays (Two-Color Microarray-Based Gene Expression Analysis). Differentially expressed genes were identified using a previously described pipeline in which data normalization is done using the Loess procedure and differential expression assessed by Limma with an adjusted $P \leq 0.05$ (Danquah et al., 2015). Data analysis (GO term enrichment) was carried out with DAVID Bioinformatics Resources (Huang et al., 2009).

For quantitative reverse transcription-PCR analysis, cDNA was synthetized from 1 $\mu$g of DNase-treated RNA using SuperScript II reverse transcriptase (Invitrogen) following the manufacturer's protocol. For reverse transcription, oligo(dT) primers were used. The SYBR FAST Universal qPCR Kit (Kapa Biosystems) was used to prepare qPCR mix. Primers (Supplemental Table S4) were used at 100 nM final concentration. Biological triplicates were performed. The following PCR program was used: 95°C for 30 s and then 40 cycles of 95°C for 5 s and 60°C for 20 s; a dissociation step also was programmed to validate the PCR products. qPCR was carried out on a CFX384 Touch Real-Time PCR device (Bio-Rad) and analyzed with CFX Manager Software (Bio-Rad).

## Metabolite Measurements

The experiment was performed in Platform Metabolism-Metabolome of the Institute of Plant Sciences Paris Saclay. To reduce the variability linked to the position of T-DNA insertion, samples were pooled from three independent *K3CA* and *K3WT* lines. Three biological replicates were done. Aerial parts were collected, and samples were lyophilized and extracted before being injected into the gas chromatography-time of flight apparatus according to the Platform Metabolism-Metabolome protocol (Tcherkez et al., 2012). SA, camalexin, and scopoletin assays were performed as described previously (Bruggeman et al., 2014).

For ethylene measurement, transgenic plants were grown in a 12-h photoperiod at 22°C on peat pellet substrate (Jiffy). At the start of the experiments, the peat pellets were treated once with NPK fertilizer (Wuxal liquid; Algukon). Light was cold white (80 $\mu$mol $m^{-2}$ $s^{-1}$). Seven- to 9-week-old plants with substrate were enclosed in a 150-mL cuvette with a flat glass lid. Cuvettes were flushed every 2 h for 20 min with synthetic air containing 350 $\mu$L $L^{-1}$ $CO_2$ (Air Liquide). Ethylene in the headspace was detected using a photoacoustic detector (ETD300; Sensor Sense; Schellingen et al., 2014). Measurements on plant-containing cuvettes were compared among them and with a cuvette containing only a peat pellet as a background control.

## Accession Numbers

Sequence data from this article can be found in the Arabidopsis Genome Initiative or GenBank/EMBL databases under the following accession numbers: At3g45640 (MPK3), At4g01370 (MPK4), At4g08480 (SUMM1), At1g12280 (SUMM2), At1g74710 (SID2), At5g03280 (EIN2), At3g26830 (PAD3), At3g13610 (F6′H1), and At2g14610 (PR1).

## Supplemental Data

The following supplemental materials are available.

**Supplemental Figure S1.** Characterization of MAPKs in *K3WT* and *K3CA* in vitro-grown plantlets in resting conditions.

**Supplemental Figure S2.** Microarray experiment overview.

**Supplemental Figure S3.** Comparison of misregulated genes in *K3CA* plants with published transcriptome.

**Supplemental Figure S4.** Ethylene-related phenotype.

**Supplemental Figure S5.** The *K3CA* autoimmune phenotype is suppressed by high temperature.

**Supplemental Figure S6.** Comparison of metabolite contents of *mips1* versus *K3CA* plants.

**Supplemental Figure S7.** Misregulated genes in *K3CA* crossed with mutants.

**Supplemental Table S1.** Transcriptome of K3WT and K3CA: list of 1,848 up-regulated genes in K3CA lines.

**Supplemental Table S2.** Transcriptome of K3WT and K3CA: list of 1,483 down-regulated genes in K3CA lines.

**Supplemental Table S3.** Transcriptome of K3WT and K3CA: GO categories for up- and down-regulated genes.

**Supplemental Table S4.** Metabolome of *K3WT*, *K3CA*, Col-0, *mpk4*, and *mips1* plants.

**Supplemental Table S5.** Primers.

## ACKNOWLEDGMENTS

We thank Yuelin Zhang and Jane Parker for *summ1/2* and *sid2* mutants, respectively, Filip Vandenbussche for ethylene measurement, and Jean Bigeard for helpful discussions and critical reading of the article.

Received March 21, 2017; accepted March 31, 2017; published April 11, 2017.

## LITERATURE CITED

**Aarts N, Metz M, Holub E, Staskawicz BJ, Daniels MJ, Parker JE** (1998) Different requirements for EDS1 and NDR1 by disease resistance genes define at least two R gene-mediated signaling pathways in *Arabidopsis*. Proc Natl Acad Sci USA **95:** 10306–10311

**Anderson JC, Bartels S, González Besteiro MA, Shahollari B, Ulm R, Peck SC** (2011) Arabidopsis MAP Kinase Phosphatase 1 (AtMKP1) negatively regulates MPK6-mediated PAMP responses and resistance against bacteria. Plant J **67:** 258–268

**Asai T, Tena G, Plotnikova J, Willmann MR, Chiu W, Gomez-Gomez L, Boller T, Ausubel FM, Sheen J** (2002) MAP kinase signalling cascade in Arabidopsis innate immunity. Nature **415:** 977–983

**Bartels S, Anderson JC, González Besteiro MA, Carreri A, Hirt H, Buchala A, Métraux JP, Peck SC, Ulm R** (2009) MAP kinase phosphatase1 and protein tyrosine phosphatase1 are repressors of salicylic acid synthesis and SNC1-mediated responses in *Arabidopsis*. Plant Cell **21:** 2884–2897

**Berriri S, Garcia AV, Frei dit Frey N, Rozhon W, Pateyron S, Leonhardt N, Montillet JL, Leung J, Hirt H, Colcombet J** (2012) Constitutively active mitogen-activated protein kinase versions reveal functions of *Arabidopsis* MPK4 in pathogen defense signaling. Plant Cell **24:** 4281–4293

**Bigeard J, Colcombet J, Hirt H** (2015) Signaling mechanisms in pattern-triggered immunity (PTI). Mol Plant **8:** 521–539

**Bigeard J, Pflieger D, Colcombet J, Gérard L, Mireau H, Hirt H** (2014) Protein complexes characterization in Arabidopsis thaliana by tandem affinity purification coupled to mass spectrometry analysis. Methods Mol Biol **1171:** 237–250

**Brodersen P, Petersen M, Nielsen HB, Zhu S, Newman MA, Shokat KM, Rietz S, Parker J, Mundy J** (2006) Arabidopsis MAP kinase 4 regulates salicylic acid- and jasmonic acid/ethylene-dependent responses via EDS1 and PAD4. Plant J **47:** 532–546

**Bruggeman Q, Garmier M, de Bont L, Soubigou-Taconnat L, Mazubert C, Benhamed M, Raynaud C, Bergounioux C, Delarue M** (2014) The polyadenylation factor subunit CLEAVAGE AND POLYADENYLATION SPECIFICITY FACTOR30: a key factor of programmed cell death and a regulator of immunity in Arabidopsis. Plant Physiol **165:** 732–746

**Bruggeman Q, Raynaud C, Benhamed M, Delarue M** (2015) To die or not to die? Lessons from lesion mimic mutants. Front Plant Sci **6:** 24

**Chong J, Baltz R, Schmitt C, Beffa R, Fritig B, Saindrenan P** (2002) Down-regulation of a pathogen-responsive tobacco UDP-Glc:phenylpropanoid glucosyltransferase reduces scopoletin glucoside accumulation, enhances oxidative stress, and weakens virus resistance. Plant Cell **14:** 1093–1107

**Clough SJ, Bent AF** (1998) Floral dip: a simplified method for Agrobacterium-mediated transformation of Arabidopsis thaliana. Plant J **16:** 735–743

**Colcombet J, Hirt H** (2008) Arabidopsis MAPKs: a complex signalling network involved in multiple biological processes. Biochem J **413:** 217–226

**Danquah A, de Zélicourt A, Boudsocq M, Neubauer J, Frei Dit Frey N, Leonhardt N, Pateyron S, Gwinner F, Tamby JP, Ortiz-Masia D, et al** (2015) Identification and characterization of an ABA-activated MAP kinase cascade in Arabidopsis thaliana. Plant J **82:** 232–244

**Daudi A, O'Brien J** (2012) Detection of hydrogen peroxide by DAB staining in Arabidopsis leaves. Bio Protoc **2:** e263

**Frei Dit Frey N, Garcia AV, Bigeard J, Zaag R, Bueso E, Garmier M, Pateyron S, de Tauzia-Moreau ML, Brunaud V, Balzergue S, et al** (2014) Functional analysis of Arabidopsis immune-related MAPKs uncovers a role for MPK3 as negative regulator of inducible defences. Genome Biol **15:** R87

**Gao M, Liu J, Bi D, Zhang Z, Cheng F, Chen S, Zhang Y** (2008) MEKK1, MKK1/MKK2 and MPK4 function together in a mitogen-activated protein kinase cascade to regulate innate immunity in plants. Cell Res **18:** 1190–1198

**Grosskinsky DK, Naseem M, Abdelmohsen UR, Plickert N, Engelke T, Griebel T, Zeier J, Novák O, Strnad M, Pfeifhofer H, et al** (2011) Cytokinins mediate resistance against Pseudomonas syringae in tobacco through increased antimicrobial phytoalexin synthesis independent of salicylic acid signaling. Plant Physiol **157:** 815–830

**Han L, Li GJ, Yang KY, Mao G, Wang R, Liu Y, Zhang S** (2010) Mitogen-activated protein kinase 3 and 6 regulate Botrytis cinerea-induced ethylene production in Arabidopsis. Plant J **64:** 114–127

**Hellens RP, Edwards EA, Leyland NR, Bean S, Mullineaux PM** (2000) pGreen: a versatile and flexible binary Ti vector for Agrobacterium-mediated plant transformation. Plant Mol Biol **42:** 819–832

**Huang W, Sherman BT, Lempicki RA** (2009) Systematic and integrative analysis of large gene lists using DAVID bioinformatics resources. Nat Protoc **4:** 44–57

**Ichimura K, Casais C, Peck SC, Shinozaki K, Shirasu K** (2006) MEKK1 is required for MPK4 activation and regulates tissue-specific and temperature-dependent cell death in Arabidopsis. J Biol Chem **281:** 36969–36976

**Ichimura K, Shinozaki K, Tena G, Sheen J, Henry Y, Champion A, Kreis M, Zhang S, Hirt H, Wilson C, et al** (2002) Mitogen-activated protein kinase cascades in plants: a new nomenclature. Trends Plant Sci **7:** 301–308

**Kai K, Shimizu B, Mizutani M, Watanabe K, Sakata K** (2006) Accumulation of coumarins in Arabidopsis thaliana. Phytochemistry **67:** 379–386

**Kong Q, Qu N, Gao M, Zhang Z, Ding X, Yang F, Li Y, Dong OX, Chen S, Li X, et al** (2012) The MEKK1-MKK1/MKK2-MPK4 kinase cascade negatively regulates immunity mediated by a mitogen-activated protein kinase kinase kinase in *Arabidopsis*. Plant Cell **24:** 2225–2236

**Lassowskat I, Böttcher C, Eschen-Lippold L, Scheel D, Lee J** (2014) Sustained mitogen-activated protein kinase activation reprograms defense metabolism and phosphoprotein profile in Arabidopsis thaliana. Front Plant Sci **5:** 554

**Liu H, Wang Y, Xu J, Su T, Liu G, Ren D** (2008) Ethylene signaling is required for the acceleration of cell death induced by the activation of AtMEK5 in Arabidopsis. Cell Res **18:** 422–432

**Liu Y, Zhang S** (2004) Phosphorylation of 1-aminocyclopropane-1-carboxylic acid synthase by MPK6, a stress-responsive mitogen-activated protein kinase, induces ethylene biosynthesis in *Arabidopsis*. Plant Cell **16:** 3386–3399

**Mao G, Meng X, Liu Y, Zheng Z, Chen Z, Zhang S** (2011) Phosphorylation of a WRKY transcription factor by two pathogen-responsive MAPKs drives phytoalexin biosynthesis in *Arabidopsis*. Plant Cell **23:** 1639–1653

**Meng PH, Raynaud C, Tcherkez G, Blanchet S, Massoud K, Domenichini S, Henry Y, Soubigou-Taconnat L, Lelarge-Trouverie C, Saindrenan P, et al** (2009) Crosstalks between myo-inositol metabolism, programmed cell death and basal immunity in Arabidopsis. PLoS ONE **4:** e7364

**Meng X, Zhang S** (2013) MAPK cascades in plant disease resistance signaling. Annu Rev Phytopathol **51:** 245–266

**Montillet J, Leonhardt N, Mondy S, Tranchimand S, Chevalier A, Castresana C, Hirt H, Laurie C** (2013) An abscisic acid-independent oxylipin pathway controls stomatal closure and immune defense in Arabidopsis. PLoS Biol **11:** e1001513

**Nakagami H, Soukupová H, Schikora A, Zárský V, Hirt H** (2006) A mitogen-activated protein kinase kinase kinase mediates reactive oxygen species homeostasis in Arabidopsis. J Biol Chem **281:** 38697–38704

**Nawrath C, Métraux JP** (1999) Salicylic acid induction-deficient mutants of *Arabidopsis* express PR-2 and PR-5 and accumulate high levels of camalexin after pathogen inoculation. Plant Cell **11:** 1393–1404

**Nitta Y, Ding P, Zhang Y** (2014) Identification of additional MAP kinases activated upon PAMP treatment. Plant Signal Behav **9:** e976155

**Nuhse T, Peck SC, Hirt H, Boller T** (2000) Microbial elicitors induce activation and dual phosphorylation of the Arabidopsis thaliana MAPK 6. J Biol Chem **275:** 7521–7526

**Park HC, Song EH, Nguyen XC, Lee K, Kim KE, Kim HS, Lee SM, Kim SH, Bae DW, Yun DJ, et al** (2011) Arabidopsis MAP kinase phosphatase 1 is phosphorylated and activated by its substrate AtMPK6. Plant Cell Rep **30:** 1523–1531

**Petersen M, Brodersen P, Naested H, Andreasson E, Lindhart U, Johansen B, Nielsen HB, Lacy M, Austin MJ, Parker JE, et al** (2000) Arabidopsis map kinase 4 negatively regulates systemic acquired resistance. Cell **103:** 1111–1120

**Pitzschke A, Djamei A, Bitton F, Hirt H** (2009) A major role of the MEKK1-MKK1/2-MPK4 pathway in ROS signalling. Mol Plant **2:** 120–137

**Qiu JL, Zhou L, Yun BW, Nielsen HB, Fiil BK, Petersen K, MacKinlay J, Loake GJ, Mundy J, Morris PC** (2008) Arabidopsis mitogen-activated protein kinase kinases MKK1 and MKK2 have overlapping functions in defense signaling mediated by MEKK1, MPK4, and MKS1. Plant Physiol **148:** 212–222

**Ranf S, Eschen-Lippold L, Pecher P, Lee J, Scheel D** (2011) Interplay between calcium signalling and early signalling elements during defence responses to microbe- or damage-associated molecular patterns. Plant J **68:** 100–113

**Ren D, Liu Y, Yang KY, Han L, Mao G, Glazebrook J, Zhang S** (2008) A fungal-responsive MAPK cascade regulates phytoalexin biosynthesis in Arabidopsis. Proc Natl Acad Sci USA **105:** 5638–5643

**Schellingen K, Van Der Straeten D, Vandenbussche F, Prinsen E, Remans T** (2014) Cadmium-induced ethylene production and responses in *Arabidopsis thaliana* rely on ACS2 and ACS6 gene expression. BMC Plant Biol **14:** 214

**Schmidt H, Günther C, Weber M, Spörlein C, Loscher S, Böttcher C, Schobert R, Clemens S** (2014) Metabolome analysis of *Arabidopsis thaliana* roots identifies a key metabolic pathway for iron acquisition. PLoS ONE **9:** e102444

**Schweighofer A, Kazanaviciute V, Scheikl E, Teige M, Doczi R, Hirt H, Schwanninger M, Kant M, Schuurink R, Mauch F, et al** (2007) The PP2C-type phosphatase AP2C1, which negatively regulates MPK4 and MPK6, modulates innate immunity, jasmonic acid, and ethylene levels in *Arabidopsis*. Plant Cell **19:** 2213–2224

**Su SH, Suarez-Rodriguez MC, Krysan P** (2007) Genetic interaction and phenotypic analysis of the Arabidopsis MAP kinase pathway mutations mekk1 and mpk4 suggests signaling pathway complexity. FEBS Lett **581:** 3171–3177

**Tcherkez G, Gúrard F, Gilard F, Lamothe M, Mauve C, Gout E, Bligny R** (2012) Metabolomic characterisation of the functional division of nitrogen metabolism in variegated leaves. Funct Plant Biol **39:** 959–967

**Tsuda K, Mine A, Bethke G, Igarashi D, Botanga CJ, Tsuda Y, Glazebrook J, Sato M, Katagiri F** (2013) Dual regulation of gene expression mediated by extended MAPK activation and salicylic acid contributes to robust innate immunity in *Arabidopsis thaliana*. PLoS Genet **9:** e1004015

**Wang H, Ngwenyama N, Liu Y, Walker JC, Zhang S** (2007) Stomatal development and patterning are regulated by environmentally responsive mitogen-activated protein kinases in *Arabidopsis*. Plant Cell **19:** 63–73

**Xu SL, Rahman A, Baskin TI, Kieber JJ** (2008) Two leucine-rich repeat receptor kinases mediate signaling, linking cell wall biosynthesis and ACC synthase in *Arabidopsis*. Plant Cell **20:** 3065–3079

**Yoo SD, Cho YH, Sheen J** (2007) Arabidopsis mesophyll protoplasts: a versatile cell system for transient gene expression analysis. Nat Protoc **2:** 1565–1572

**Zhang Z, Wu Y, Gao M, Zhang J, Kong Q, Liu Y, Ba H, Zhou J, Zhang Y** (2012) Disruption of PAMP-induced MAP kinase cascade by a Pseudomonas syringae effector activates plant immunity mediated by the NB-LRR protein SUMM2. Cell Host Microbe **11:** 253–263